



HAL
open science

Analysis of potential locations of asteroidal moonlets

Hexi Baoyin, Xiaodong Liu, Laurène Beauvalet

► **To cite this version:**

Hexi Baoyin, Xiaodong Liu, Laurène Beauvalet. Analysis of potential locations of asteroidal moonlets. Monthly Notices of the Royal Astronomical Society, 2013, <http://mnras.oxfordjournals.org/content/430/4/3483.full.pdf>. 10.1093/mnras/stt149 . hal-01182985

HAL Id: hal-01182985

<https://hal.science/hal-01182985>

Submitted on 5 Aug 2015

HAL is a multi-disciplinary open access archive for the deposit and dissemination of scientific research documents, whether they are published or not. The documents may come from teaching and research institutions in France or abroad, or from public or private research centers.

L'archive ouverte pluridisciplinaire **HAL**, est destinée au dépôt et à la diffusion de documents scientifiques de niveau recherche, publiés ou non, émanant des établissements d'enseignement et de recherche français ou étrangers, des laboratoires publics ou privés.

Analysis of potential locations of asteroidal moonlets[★]

Hexi Baoyin,¹† Xiaodong Liu¹ and Laurène Beauvalet²

¹*School of Aerospace, Tsinghua University, Beijing 100084, China*

²*IMCCE-Observatoire de Paris, 77, avenue Denfert-Rochereau, F-75014 Paris, France*

Accepted 2013 January 23. Received 2012 December 16; in original form 2012 October 12

ABSTRACT

In this study, the potential locations of asteroidal small satellites (also called moonlets) with quasi-circular mutual orbit are analysed. For the motion of the moonlets, only the solar gravity perturbation and the primary's second degree-and-order gravity field are considered. By eliminating short periodic terms, the dynamical behaviour of the Hamiltonian for the moonlets is investigated. The observational data of some high-size-ratio binary asteroids show that the orbits of the moonlets lie close to the classical Laplace equilibrium points, which reach global minimum values of the Hamiltonian. It is found that tides or Yarkovsky effects alone cannot account for the reason why the orbits of asteroidal moonlets are not exactly at the classical Laplace equilibrium points. The analysis in this study is expected to provide useful information for the potential locations of asteroidal moonlets, and contribute to principles to relate predictions to observations.

Key words: celestial mechanics – minor planets, asteroids: general.

1 INTRODUCTION

Binary minor planets are recent discoveries. The first confirmed binary asteroids 243 Ida-Dactyl were discovered in 1993 (Belton et al. 1995, 1996; Chapman et al. 1995). The investigations of binary minor planets have aroused great interest (Richardson & Walsh 2006). A comprehensive online data base for binary asteroid systems is available on web page <http://www.asu.cas.cz/~asteroid/binastdata.htm>, the construction of which is described in Pravec & Harris (2007) and Pravec et al. (2012).

For the dynamics of binary asteroid systems, some work has been done in previous studies. The generalized Tisserand constant was used to elucidate orbital dynamical properties of distant moons of asteroids (Hamilton & Krivov 1997). In order to study the stability of the binary asteroids, the system was modelled based on the full two-body problem (Scheeres 2002a,b, 2004, 2006, 2007, 2009; Breiter et al. 2005; Fahnestock & Scheeres 2006). A two-dimensional dynamical model of the binary asteroids including primary's oblateness, solar perturbations and the BYORP (binary Yarkovsky-O'Keefe-Radzievskii-Paddack) effect enabled to obtain new results about orbital evolution (Čuk & Nesvorný 2010). Numerical simulations were applied to investigate the stability of the binary asteroids 243 Ida (Petit et al. 1997), and the triple asteroids 87 Sylvania (Winter et al 2009; Frouard & Compère 2012). Both the sta-

bility regions around the triple asteroids 2001 SN263 (Araujo et al. 2012) and the collisionally born family about 87 Sylvania were also investigated using numerical models and integrations (Vokrouhlický et al. 2010). The Hill stability of binary minor planets was discussed using the total angular momentum and the total energy of the system (Donnison 2011). In our previous study, the Hill stability of triple minor planets was also examined (Liu et al. 2012). Scheeres et al. (2006) and Fahnestock & Scheeres (2008) studied dynamics of the near-Earth binary asteroids 1999 KW4. Fang et al. (2011) analysed several processes that can excite the observed eccentricity and inclinations for near-Earth triple asteroids 2001 SN263 and 1994 CC. Further, Fang & Margot (2012) investigated the evolutionary mechanisms that can explain the origin of the spin with orbital parameters for near-Earth binaries and triples. Besides, there are plenty of papers on dynamics of a particle around an asteroid (Hamilton & Burns 1991, 1992; Chauvineau, Farinella & Mignard 1993; Scheeres 1994; Scheeres et al. 1996; Rossi, Marzari & Farinella 1999; Scheeres, Williams & Miller 2000; Vasilkova 2005; Colombi, Hirani & Villac 2008; Yu & Baoyin 2012), which can also be applied to asteroidal moonlets.

The relevance of the dynamical behaviour of asteroidal moonlets to the Laplace plane is studied in this study. Laplace (1805) introduced the concept of the Laplace plane of a planetary satellite.¹ For a satellite with circular orbit influenced by the planetary oblateness and the solar gravity perturbation, the Laplace plane is defined as the plane around which the instantaneous orbital plane of the

[★]Some parts of the manuscript presented at the 63rd International Astronomical Congress, in Naples, Italy, 2012 October 1–5. www.iafastro.org

† E-mail: baoyin@tsinghua.edu.cn

¹ Sometimes, the term Laplace plane is used to refer to the invariable plane, the plane perpendicular to the angular momentum vector of the entire system.

satellite precesses. The Laplace plane possesses a constant inclination with respect to the planetary equatorial plane. The classical Laplace plane's axis is coplanar with and between the planet's spin axis and the planet's heliocentric orbit axis. In many works, dynamics of planetary satellites on the Laplace plane were studied. Allan & Cook (1964) found that for a circular orbit with given size, three mutually perpendicular directions in which the axis of the orbit remains stationary exist: two stable and one unstable. One of the stable directions corresponds to the classical Laplace plane. Ward (1981) showed that circumplanetary disc's structure could affect the orientation of the local Laplacian plane. Stable rings are possible to exist in the circular orthogonal Laplace equilibrium points (Dobrovolskis 1980; Borderies 1989; Dobrovolskis, Steiman-Cameron & Borderies 1989a; Dobrovolskis, Borderies & Steiman-Cameron 1989b). Dobrovolskis (1993) studied the maps of Laplace planes for Uranus and Pluto, which are helpful for new satellites searches. Kudielka (1994) found that 'balanced' Earth satellites' orbits exist both in the classical Laplace plane and in the plane perpendicular to the classical Laplace plane. Tremaine, Touma & Namouni (2009) presented a comprehensive study of the Laplace equilibrium points including the effect of eccentricity. By truncating the gravitational potential up to the second order, Boué & Laskar (2006) presented the application of the Laplace plane to a three-body system consisting of a central star, an oblate planet and a satellite orbiting the planet. Most of the previous papers focused on the application of the Laplace plane to planetary satellites. Considering the interactions of two rigid bodies, the concept of the Laplace plane was applied to binary asteroids to analyse the full coupled rotational and translational dynamics (Fahnestock & Scheeres 2008; Boué & Laskar 2009). In Fahnestock & Scheeres (2008), the gravitational potential was expanded up to the second order, whereas in Boué & Laskar (2009), the gravitational potential was further expanded up to the fourth order.

Some high-size-ratio binary asteroids in the Solar system are found to possess quasi-circular mutual orbits, for example, 22 Kalliope, 45 Eugenia, 87 Sylvia, 107 Camilla, 121 Hermione, 216 Kleopatra. Recent studies were ever performed on the high-size-ratio binary asteroids. Four high-size-ratio main-belt binary asteroids with quasi-circular mutual orbits were focused on in Marchis et al. (2008). The evolution of the high size binary asteroids was studied using the MEGNO indicator (Mean Exponential Growth Factor of Nearby Orbits) and the truncated potential up to the second degree-and-order in Compère, Lemaître & Delsate (2011). In this paper, only high-size-ratio binary asteroids with quasi-circular mutual orbits are considered, and simple model is used. People who are interested in more complicated models can refer to Boué & Laskar (2009) and Fahnestock & Scheeres (2008), which contributed significantly to the modelling of the binary asteroids. The analysis in this study is expected to provide a priori knowledge for the potential locations of asteroidal moonlets, and contribute to principles to relate predictions to observations.

2 THE SECULAR DISTURBING FUNCTION DUE TO THE SOLAR GRAVITY PERTURBATION AND THE PRIMARY'S NON-SPHERICITY

In this study, we are concerned with high-size-ratio binary asteroids with quasi-circular mutual orbits. The eccentricity of the mutual orbits is assumed zero. The moonlet's effect on other bodies of the system is assumed negligible. This hypothesis comes from the fact that the moonlet's mass is expected to be too small to be detected,

and as such, too small to have any major influence on the dynamics of the primary, which would end only in a very slight perturbation of the primary's heliocentric distance, and as such, a very small change in the solar gravity perturbation. In all the dynamical studies of such systems, as those of 45 Eugenia in Marchis et al. (2010) for example, the masses of the satellites have not been determined, but estimated from hypothesis on their density and size. Since the geometry of the moonlet would have an even smaller effect than the effect of its centre of mass, we also do not take into account the shape of the moonlet. The orbit of the moonlet is under the influence of a variety of perturbations: the solar gravity perturbation, the solar radiation pressure, the gravitational harmonics of the primary, etc. The effects of these perturbations were analysed in the previous research presented in the following. The solar-radiation pressure affects significantly for very small particles, but slightly affects particles larger than a few centimetres (Hamilton & Burns 1992; Scheeres 1994). The gravitational harmonics dominate when close to the asteroid (Scheeres 1994). The solar gravity perturbation dominates when fairly far from the asteroid (Hamilton & Burns 1991; Scheeres 1994), and is important for the long-term evolution of the satellites (Yokoyama 1999). Thus, for the moonlet's motion, only the solar gravity perturbation and the non-spherical effect of the primary are considered. Further, we only consider the second degree-and-order gravitational harmonics for the non-spherical effect of the primary because of the large primary-moonlet separations with respect to the primary's radii. For simplicity, the mutual perturbations between moonlets are neglected if there are more than one moonlets in the system, the secular effects of which due to a secular resonance have been analysed in Winter et al. (2009).

In this paper, the primary's heliocentric orbital plane is taken as the reference plane. The perturbation due to the second degree-and-order gravity field from the primary is averaged with respect to both the primary's spin period and the moonlet's orbital period. The secular part of the disturbing function R_p due to the primary's second degree-and-order gravity field in the primary's heliocentric orbital plane is obtained as (Kinoshita & Nakai 1991; Domingos, Moraes & Prado 2008; Tremaine et al. 2009)

$$R_p = n_p^2 J_2 R_e^2 [3(\cos i \cos \varepsilon + \sin i \sin \varepsilon \cos \Omega)^2 - 1] / 4, \quad (1)$$

where n_p is the mean motion of the moonlet, J_2 is the oblateness coefficient, R_e is the reference radius of the primary, i is inclination, ε is the inclination of the primary's equatorial plane with respect to the primary's heliocentric orbital plane and Ω is right ascension of the ascending node. Note that the gravity harmonic J_{22} is eliminated by averaging over the primary's spin period. The solar gravity perturbation is averaged with respect to both the primary's heliocentric orbital period and the moonlet's orbital period. The secular part of the disturbing function R_\odot due to the solar gravity perturbation is (Kinoshita & Nakai 1991; Domingos et al. 2008; Tremaine et al. 2009)

$$R_\odot = m_\odot n_\odot^2 a^2 (3 \cos^2 i - 1) / [8(m_p + m_\odot)(1 - e_\odot^2)^{3/2}], \quad (2)$$

where m_\odot is the mass of the Sun, n_\odot is the mean motion of the Sun, a is the moonlet's semimajor axis, m_p is the mass of the primary and e_\odot is the primary's heliocentric orbital eccentricity. The secular part of the disturbing function R due to both perturbations is presented as

$$R = R_\odot + R_p. \quad (3)$$

3 THE FROZEN SOLUTIONS IN THE PRIMARY'S HELIOCENTRIC ORBITAL PLANE

Based on the Lagrange's planetary equations (Chobotov 2002, p. 201), the variation rates of i and Ω can be easily derived as (Liu & Ma 2012)

$$\frac{di}{dt} = \frac{3n_p J_2 R_e^2}{2a^2} \sin \Omega \sin \varepsilon (\cos i \cos \varepsilon + \sin i \sin \varepsilon \cos \Omega), \quad (4)$$

$$\frac{d\Omega}{dt} = -\frac{3m_\odot n_\odot^2 \cos i}{4n_p (m_p + m_\odot) (1 - e_\odot^2)^{3/2}} - \frac{3n_p J_2 R_e^2}{4a^2 \sin i} \times (-\sin 2i \cos^2 \varepsilon + \sin 2i \sin^2 \varepsilon \cos^2 \Omega + \cos 2i \sin 2\varepsilon \cos \Omega). \quad (5)$$

For circular or quasi-circular moonlet's orbits, it is obvious that the Delaunay variables $L = G = \sqrt{\mu_p a}$ are constant. Thus, the averaged system has only one degree of freedom in (H, Ω) , where $H = G \cos i$ (Murray & Dermott 1999, p. 59). Since G is constant, the orbital parameters (i, Ω) are used instead of the Delaunay variables (H, Ω) . It is evident from equation (4) that there exist the frozen solutions when $\Omega = 0^\circ$ (or 180°), which are the circular coplanar Laplace equilibrium points according to Tremaine et al. (2009). The values of these frozen i for the Laplace equilibrium points can be solved numerically by setting the right-hand side of equation (5) equal to zero. Because either $\cos i$ or $\cos \Omega$ exist in the right-hand sides of both equations (4) and (5), another two frozen solutions exist: $\Omega = \pm 90^\circ$ and $i = 90^\circ$, which are the circular orthogonal Laplace equilibrium points according to Tremaine et al. (2009). The linear stability of the Laplace equilibrium points including the oblateness and the solar gravity perturbation was examined using the vector description by Tremaine et al. (2009). In this paper, the stability of the Laplace equilibrium points to variations in i and Ω is determined by analysing the characteristic equation of the linearized model of equations (4) and (5). By defining a vector $\mathbf{X} = (\delta i, \delta \Omega)^T$ as the variations, the variational equations of equations (4) and (5) are written as

$$\dot{\mathbf{X}} = \mathbf{A} \cdot \mathbf{X}, \quad (6)$$

where

$$\mathbf{A} = \begin{bmatrix} \frac{\partial(di/dr)}{\partial i} & \frac{\partial(di/dr)}{\partial \Omega} \\ \frac{\partial(d\Omega/dr)}{\partial i} & \frac{\partial(d\Omega/dr)}{\partial \Omega} \end{bmatrix}.$$

The characteristic equation of equation (6) for the circular orthogonal Laplace equilibrium is calculated as

$$\lambda^2 = -\frac{9\mu' n_\odot^2 \sin^2 \varepsilon J_2 R_e^2}{8a^2 (1 - e_\odot^2)^{3/2}}. \quad (7)$$

If $\lambda^2 > 0$, which means that one eigenvalue of \mathbf{A} is a positive real number, so the Laplace equilibrium is unstable; if $\lambda^2 < 0$, both eigenvalues are pure imaginary, which means that the elements i and Ω are both oscillatory, so the Laplace equilibrium is linearly stable. For some actual asteroidal moonlets, the examinations of stability to variations in i and Ω will be also presented in Section 5.

4 NUMERICAL VERIFICATION

In this section, the averaged model is applied to 22 Kalliope's moonlet Linus for verification. The averaged results are compared to the

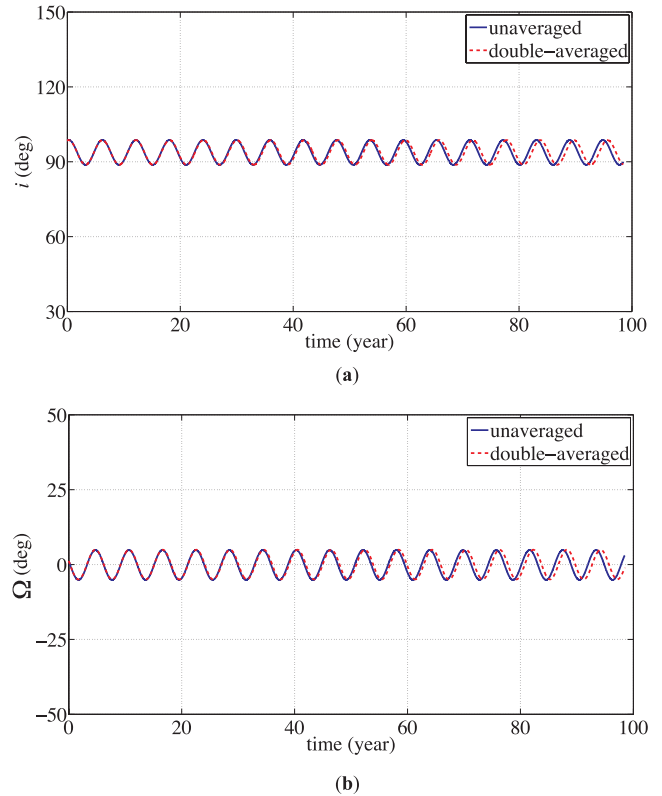


Figure 1. Evolutions of Linus's orbital elements over 10 000 T_s . The solid line in blue corresponds to results of the direct numerical simulations of the full (unaveraged) equations of motion; the dashed lines in red correspond to results of the averaged model. (a) Evolution of i over 10 000 T_s . (b) Evolution of Ω over 10 000 T_s .

direct numerical simulations of the full equations of motion including the unaveraged solar gravity perturbation and the unaveraged primary's second degree-and-order gravity field. The orbital parameters of the primary in the J2000 ecliptic coordinate system are available from the JPL Horizon service. The orbital elements of the moonlet in the J2000 Earth equatorial-coordinate frame adopted in this paper are from Vachier, Berthier & Marchis (2012). The derived spin vector solution of the primary in J2000 ecliptic coordinates is taken from Descamps et al. (2008). The primary's heliocentric orbital plane is adopted as the reference plane. The duration time of the orbital evolution is set to 10 000 T_s .

The evolutions of the moonlet's orbital elements are presented in Fig. 1. It can be seen that the results of the averaged models show a satisfactory approximation to those of the unaveraged model for inclination i and right ascension of the ascending node Ω . Those two results are almost overlaid with each other. The mean Ω is about 0° and the mean i is about 93.7° , which meets the frozen condition discussed in Section 3.

5 ANALYSIS OF LOCATIONS OF ASTEROIDAL MOONLETS

After averaging, the Hamiltonian can be presented as follows

$$\mathcal{H} = -\mu_p/2a - R. \quad (8)$$

It is obvious that the averaged Hamiltonian is time independent for asteroidal moonlets with quasi-circular orbits, so the averaged Hamiltonian is an integral constant and represents the energy of the averaged system. Define the Hessian matrix \mathbf{H}_s ,

$$\mathbf{H}_s = \begin{bmatrix} \frac{\partial^2 \mathcal{H}}{\partial i^2} & \frac{\partial^2 \mathcal{H}}{\partial i \partial \Omega} \\ \frac{\partial^2 \mathcal{H}}{\partial \Omega \partial i} & \frac{\partial^2 \mathcal{H}}{\partial \Omega^2} \end{bmatrix}. \tag{9}$$

If \mathbf{H}_s is positive definite at the Laplace equilibrium, then the Hamiltonian \mathcal{H} attains a local minimum at this equilibrium. If \mathbf{H}_s is negative definite at the Laplace equilibrium, then \mathcal{H} attains a local maximum at this equilibrium.

Several asteroidal moonlets 22 Kalliope’s moonlet Linus, 121 Hermione’s moonlet S/2001 (121) 1, 45 Eugenia’s moonlets Petit-Prince and Petite-Princesse, and 216 Kleopatra’s moonlets S/2008 (216) 1 and S/2008 (216) 2 are taken as examples to analyse the behaviours of the Hamiltonian in the parameter plane of i and Ω . The eccentricity for the moonlet’s orbit is kept equal to zero, and the semimajor axis for the moonlet’s orbit is kept as its actual value. The orbital parameters of Linus, S/2001 (121) 1, Petit-Prince, Petite-Princesse, S/2008 (216) 1 and S/2008 (216) 2 are taken from Vachier et al. (2012), Descamps et al. (2009), Beauvalet et al. (2011), Beauvalet et al. (2011), Descamps et al. (2011) and Descamps et al. (2011), respectively. These moonlets’ orbits are all almost circular. The spin vector solutions of the primaries 22 Kalliope, 121 Hermione, 45 Eugenia and 216 Kleopatra are taken from Descamps et al. (2008), Descamps et al. (2009), Beauvalet et al. (2011) and Descamps et al. (2011), respectively. For the primary 22 Kalliope, $J_2 = 0.19$ (Descamps et al. 2008); for 121 Hermione, $J_2 = 0.28$ (Descamps et al. 2009); for 45 Eugenia, $J_2 = 0.060$ (Marchis et al. 2010) and for 216 Kleopatra, $J_2 = 0.6$ (Descamps et al. 2011). It can be seen that the primary’s J_2 is much larger than Earth’s $J_2 = 1.082\ 63 \times 10^{-3}$ (Lemoine et al. 1998) and Martian $J_2 = 1.955\ 45 \times 10^{-3}$ (Lemoine et al. 2001). Simulations of 22 Kalliope’s moonlet Linus, 121 Hermione’s moonlet S/2001 (121) 1, 45 Eugenia’s moonlets Petit-Prince and Petite-Princesse, and 216 Kleopatra’s moonlets S/2008 (216) 1 and S/2008 (216) 2 are shown in Figs 2–7, respectively.

It is evident in Fig. 2 that six Laplace equilibrium points are found in total in the range of $i \in [0, 180^\circ]$ and $\Omega \in [-180^\circ, 180^\circ]$ for 22 Kalliope’s moonlet Linus. The values of the frozen i and Ω at these

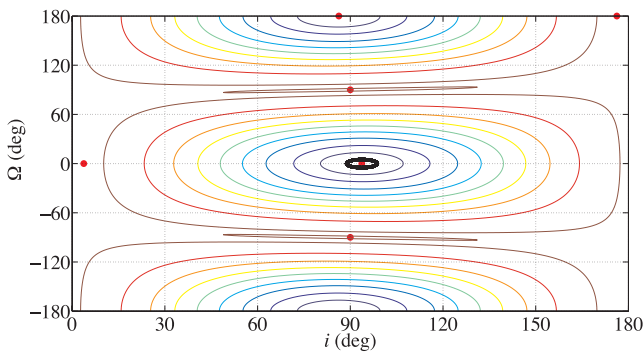


Figure 2. Contours of the averaged Hamiltonian \mathcal{H} in the parameter plane of i and Ω for 22 Kalliope’s moonlet Linus. The thicker line in black corresponds to Petite-Princesse’s orbit of 10 000 T_s . The red dots correspond to the Laplace equilibrium points.

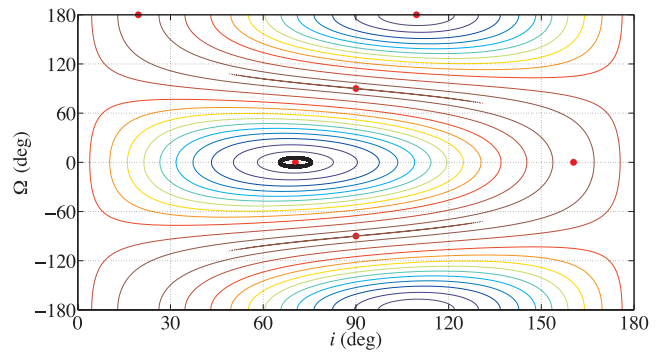


Figure 3. Contours of the averaged Hamiltonian \mathcal{H} in the parameter plane of i and Ω for 121 Hermione’s moonlet S/2001 (121) 1. The thicker line in black corresponds to S/2001 (121) 1’s orbit of 10 000 T_s . The red dots correspond to the Laplace equilibrium points.

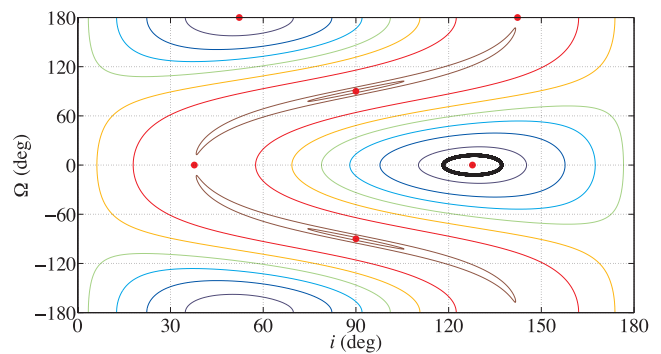


Figure 4. Contours of the averaged Hamiltonian \mathcal{H} in the parameter plane of i and Ω for 45 Eugenia’s moonlet Petit-Prince. The thicker line in black corresponds to Petit-Prince’s orbit of 10 000 T_s . The red dots correspond to the Laplace equilibrium points.

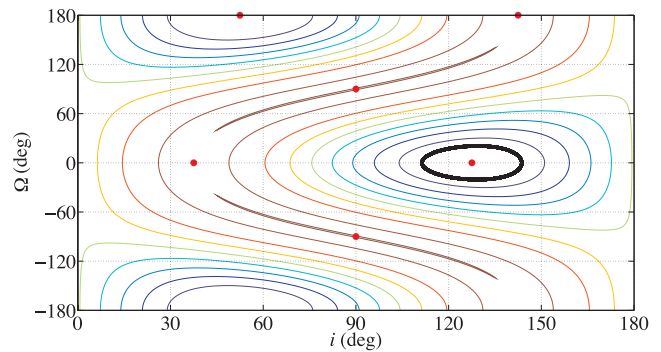


Figure 5. Contours of the averaged Hamiltonian \mathcal{H} in the parameter plane of i and Ω for 45 Eugenia’s moonlet Petite-Princesse. The thicker line in black corresponds to Petite-Princesse’s orbit of 10 000 T_s . The red dots correspond to the Laplace equilibrium points.

Laplace equilibrium points can be obtained by solving equilibrium solutions of equations (4) and (5), which are shown as follows:

$$\begin{aligned} &(\Omega = 90^\circ, i = 90^\circ); \quad (\Omega = -90^\circ, i = 90^\circ); \\ &(\Omega = 0^\circ, i = 93^\circ.74); \quad (\Omega = 180^\circ, i = 86^\circ.26); \\ &(\Omega = 0^\circ, i = 3^\circ.74); \quad (\Omega = 180^\circ, i = 176^\circ.26). \end{aligned}$$

According to Tremaine et al. (2009), the equilibrium points when $i = 90^\circ$ are the circular orthogonal Laplace equilibrium points, and the other four equilibrium points are the circular coplanar Laplace

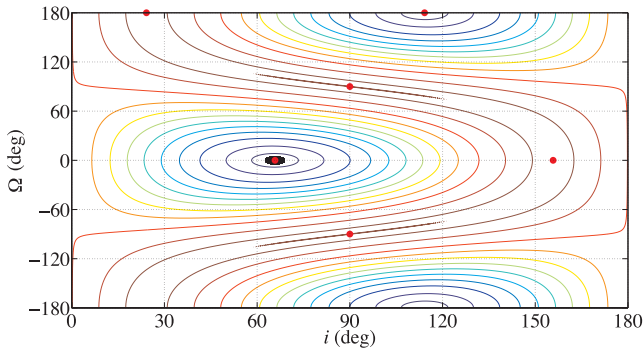


Figure 6. Contours of the averaged Hamiltonian \mathcal{H} in the parameter plane of i and Ω for 216 Kleopatra's moonlet S/2008 (216) 1. The thicker line in black corresponds to Petite-Princesse's orbit of $10\,000 T_s$. The red dots correspond to the Laplace equilibrium points.

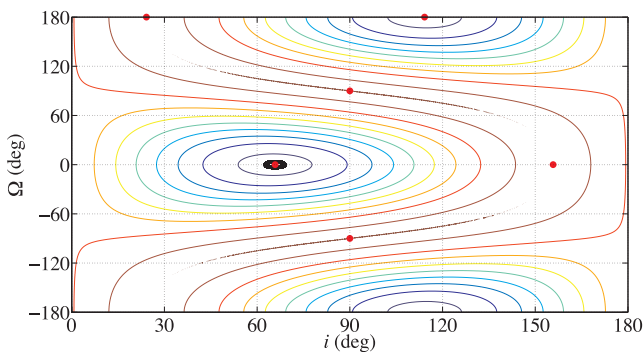


Figure 7. Contours of the averaged Hamiltonian \mathcal{H} in the parameter plane of i and Ω for 216 Kleopatra's moonlet S/2008 (216) 2. The thicker line in black corresponds to Petite-Princesse's orbit of $10\,000 T_s$. The red dots correspond to the Laplace equilibrium points.

equilibrium points. For the first four Laplace equilibrium points, the eigenvalues of equation (6) are all pure imaginary according to equation (7), so the elements i and Ω are all oscillatory. Thus, these four Laplace equilibrium points are all linearly stable to variations in i and Ω . For other two Laplace equilibrium points, one of the eigenvalues of equation (6) is a positive real number, so they are unstable to variations in i and Ω . Based on equation (9), the extremum properties of the linearly stable Laplace equilibrium points are examined. For the circular coplanar Laplace equilibrium points, the Hessian matrix \mathbf{H}_s is negative definite according to equation (9), so the Hamiltonian \mathcal{H} attains a local maximum at these equilibrium points. For the classical Laplace equilibrium ($\Omega = 0^\circ, i = 93^\circ.74$) and the other circular coplanar linearly stable Laplace equilibrium ($\Omega = 180^\circ, i = 86^\circ.26$), \mathbf{H}_s is positive definite, so the Hamiltonian \mathcal{H} attains a local minimum.

Seen from Figs 3–7, there are also six Laplace equilibrium points for 121 Hermione's moonlet S/2001 (121) 1, 45 Eugenia's moonlets Petite-Prince and Petite-Princesse, and 216 Kleopatra's moonlets S/2008 (216) 1 and S/2008 (216) 2: two linearly stable equilibrium points with local minimum values of the Hamiltonian, two linearly stable equilibrium points with local maximum values of the Hamiltonian and two unstable equilibrium points. It is noted from Figs 2–7 that the orbits of these actual asteroidal moonlets all lie close to the classical Laplace equilibrium points that reach global minimum values of the Hamiltonian \mathcal{H} , which means that the normal of the averaged moonlet's orbital plane, the primary's spin axis and the normal of the primary's heliocentric orbital plane are approximately

coplanar. The reason why the orbits of asteroidal moonlets are not exactly at the classical Laplace equilibrium points might be due to the effect of the other perturbations. Yet, our knowledge of the dissipative forces in these kinds of systems suggests that tides or Yarkovsky effects alone cannot account for this. If we consider the tidal effects between 45 Eugenia and Petit-Prince, the primary's tidal Love number k_p of 45 Eugenia is expected to be given by (Goldreich & Sari 2009),

$$k_p \approx 10^{-5} \frac{R_e}{1 \text{ km}}. \quad (10)$$

If we suppose that Petit-Prince is in a spin–orbit resonance with respect to 45 Eugenia, we can then have an estimation of its semi-major axis changing rate (Goldreich & Sari 2009),

$$\frac{1}{a} \frac{da}{dt} = 3 \frac{k_p}{Q_p} \frac{m_m}{m_p} \left(\frac{R_e}{a} \right)^5 n_p, \quad (11)$$

where Q_p is tidal quality factor, and m_m is the mass of the moonlets. Since here we are studying the tidal evolution of the moonlet, we have to make a few assumptions on its mass.

This formula gives a semimajor axis changing rate of about 4 m per century, far from enough to explain a drift from the equilibrium point if the satellite has been captured or formed there. It can also be seen from here that the effect of the Petite-Prince's mass on the mutual orbit is marginal. Concerning the Yarkovsky effect, we can compare the satellites of 45 Eugenia to those of Mars. This effect depends mainly on the distance between the Sun and the small objects considered. In the case of Phobos and Deimos, the diurnal Yarkovsky effect is negligible on the evolution of the satellites, a few centimetres of semimajor axis change on one million years (Tajeddine, Lainey & Hestroffer 2011). 45 Eugenia being even farther from the Sun, we can safely neglect the Yarkovsky effect on the evolution of 45 Eugenia's satellites. The mechanism preventing the satellites from reaching the equilibrium points, or drifting them from it, is still to be determined, but their proximity to these points is a clear indication that these points are still important in the dynamics of the satellites and are good approximation of their position.

6 CONCLUSIONS

In this study, the potential locations of asteroidal moonlets with quasi-circular mutual orbit are investigated. By analysing frozen solutions of the averaged equations of motion, we found that the orbits of several actual moonlets lie close to one type of frozen solutions that are called the classical Laplace equilibrium points. The normal of the mean orbital plane of the moonlet, the primary's spin axis and the normal of the primary's heliocentric orbital plane are found to be approximately coplanar, which is generally consistent with the previous studies (Fahnestock & Scheeres 2008; Boué & Laskar 2009). Even though no clear mechanism can explain the small difference between the satellites' current position and the equilibrium points, they are good enough approximation for the satellites position. The positions of these points do not depend on any a priori hypothesis on the moonlet's shape or mass apart from the fact that its mass is negligible with respect to the primary.

To determine those equilibrium positions, we need to know the orientation of the primary's spin pole, the primary's mass, the J_2 coefficient and the moonlet's orbital size. The orientation of the primary's spin pole can be estimated from light-curve inversion in the case of 45 Eugenia for example (Taylor et al. 1988). Prior to the discovery of a satellite or a probe's fly-by, there is no possibility to

determine precisely the mass of the primary. Yet, from the spectra, we can make assumptions on the primary's density and hence its mass. Its light curve can then provide its shape (Carry et al. 2012) and its polar oblateness (Turcotte & Schubert 2002). Most high-ratio systems being compact, we can assume that the satellite would be at most at a distance of a few per cent of the primary's Hill radius. A supposed semimajor axis in this range would then be a good first approximation. A systematic investigation around these equilibrium points may then lead us to discover these satellites.

ACKNOWLEDGEMENTS

This work was supported by National Basic Research Program of China (973 Program) (2012CB720000) and the National Natural Science Foundation of China (No. 11072122).

REFERENCES

- Allan R. R., Cook G. E., 1964, *Proc. R. Soc. A*, 280, 97
 Araujo R. A. N., Winter O. C., Prado A. F. B. A., Sukhanov A., 2012, *MNRAS*, 423, 3058
 Beauvalet L., Marchis F., Lainey V., Allain M., 2011, EPSC-DPS Joint Meeting, Nantes, France, p. 728
 Belton M. J. S. et al., 1995, *Nat*, 374, 785
 Belton M. J. S. et al., 1996, *Icarus*, 120, 185
 Borderies N., 1989, *Icarus*, 77, 135
 Boué G., Laskar J., 2006, *Icarus*, 185, 312
 Boué G., Laskar J., 2009, *Icarus*, 201, 750
 Breiter S., Melendo B., Bartczak P., Wyrzyszczyk I., 2005, *A&A*, 437, 753
 Carry B. et al., 2012, *Planet. Space Sci.*, 66, 200
 Chapman C. R. et al., 1995, *Nat*, 374, 783
 Chauvineau B., Farinella P., Mignard F., 1993, *Icarus*, 105, 370
 Chobotov V. A., 2002, *Orbital Mechanics*, 3rd edn., AIAA, Reston, VA
 Colombi A., Hirani A. N., Villac B. F., 2008, *J. Guid. Control Dyn.*, 31, 1041
 Compère A., Lemaître A., Delsate N., 2011, *Celest. Mech. Dyn. Astron.*, 112, 75
 Čuk M., Nesvorný M., 2010, *Icarus*, 207, 732
 Descamps P. et al., 2008, *Icarus*, 196, 578
 Descamps P. et al., 2009, *Icarus*, 203, 88
 Descamps P. et al., 2011, *Icarus*, 211, 1022
 Dobrovolskis A. R., 1980, *Icarus*, 43, 222
 Dobrovolskis A. R., 1993, *Icarus*, 105, 400
 Dobrovolskis A. R., Steiman-Cameron T. Y., Borderies N. L., 1989a, *Geophys. Res. Lett.*, 16, 949
 Dobrovolskis A. R., Borderies N. L., Steiman-Cameron T. Y., 1989b, *Icarus*, 81, 132
 Domingos R. C., Moraes R. V., Prado A. F. B. A., 2008, *Math. Probl. Eng.*, 2008, 763654
 Donnison J. R., 2011, *MNRAS*, 415, 470
 Fahnestock E. G., Scheeres D. J., 2006, *Celest. Mech. Dyn. Astron.*, 96, 317
 Fahnestock E. G., Scheeres D. J., 2008, *Icarus*, 194, 410
 Fang J., Margot J.-L., 2012, *AJ*, 143, 24
 Fang J., Margot J.-L., Brozovic M., Nolan M. C., Benner L. A. M., Taylor P. A., 2011, *AJ*, 141, 154
 Frouard J., Compère A., 2012, *Icarus*, 220, 149
 Goldreich P., Sari R., 2009, *ApJ*, 691, 54
 Hamilton D. P., Burns J. A., 1991, *Icarus*, 92, 118
 Hamilton D. P., Burns J. A., 1992, *Icarus*, 96, 43
 Hamilton D. P., Krivov A. V., 1997, *Icarus*, 128, 241
 Kinoshita H., Nakai H., 1991, *Celest. Mech. Dyn. Astron.*, 52, 293
 Kudielka V., 1994, *Celest. Mech. Dyn. Astron.*, 60, 445
 Laplace P. S., 1805, *Mécanique Céleste*. Courcier, Paris
 Lemoine F. G. et al., 1998, NASA TM-1998-206861
 Lemoine F. G., Smith D. E., Rowlands D. D., Zuber M. T., Neumann G. A., Chinn D. S., Pavlis D. E., 2001, *J. Geophys. Res.*, 106, 23359
 Liu X., Baoyin H., Georgakarakos N., Donnison J. R., Ma X., 2012, *MNRAS*, 427, 1034
 Liu X., Ma X., 2012, 63rd Int. Astron. Congr., Naples, Italy
 Marchis F., Descamps P., Baek M., Harris A. W., Kaasalainen M., Berthier J., Hestroffer D., Vachier F., 2008, *Icarus*, 196, 97
 Marchis F. et al., 2010, *Icarus*, 210, 635
 Murray C. D., Dermott S. F., 1999, *Solar System Dynamics*. Cambridge Univ. Press, Cambridge
 Petit J.-M., Durda D. D., Greenberg R., Hurford T. A., Geissler P. E., 1997, *Icarus*, 130, 177
 Pravec P., Harris A. W., 2007, *Icarus*, 190, 250
 Pravec P. et al., 2012, *Icarus*, 218, 125
 Richardson D. C., Walsh K. J., 2006, *Annu. Rev. Earth Planet. Sci.*, 34, 47
 Rossi A., Marzari F., Farinella P., 1999, *Earth Planets Space*, 51, 1173
 Scheeres D. J., 1994, *Icarus*, 110, 225
 Scheeres D. J., 2002a, *Celest. Mech. Dyn. Astron.*, 83, 155
 Scheeres D. J., 2002b, *Icarus*, 159, 271
 Scheeres D. J., 2004, *Ann. New York Acad. Sci.*, 1017, 81
 Scheeres D. J., 2006, *Celest. Mech. Dyn. Astron.*, 94, 317
 Scheeres D. J., 2007, in Milani A., Valsecchi G. B., Vokrouhlický D., eds, *Proc. IAU Symp. 236, Near Earth Objects, Our Celestial Neighbors: Opportunity and Risk*. Cambridge Univ. Press, Cambridge, p. 177
 Scheeres D. J., 2009, *Celest. Mech. Dyn. Astron.*, 104, 103
 Scheeres D. J., Ostro S. J., Hudson R. S., Werner R. A., 1996, *Icarus*, 121, 67
 Scheeres D. J., Williams B. G., Miller J. K., 2000, *J. Guid. Control Dyn.*, 23, 466
 Scheeres D. J. et al., 2006, *Sci*, 314, 1280
 Tajeddine R., Lainey V., Hestroffer D., 2011, EPSC-DPS Joint Meeting, Nantes, France, p. 859
 Taylor R. C., Birch P. V., Pospieszalska-Surdej A., Surdej J., 1988, *Icarus*, 73, 314
 Tremaine S., Touma J., Namouni F., 2009, *AJ*, 137, 3706
 Turcotte D. L., Schubert G., 2002, *Geodynamics*, 2nd edn. Cambridge Univ. Press, Cambridge
 Vachier F., Berthier J., Marchis F., 2012, *A&A*, 543, A68
 Vasilkova O., 2005, *A&A*, 430, 713
 Vokrouhlický D. et al., 2010, *AJ*, 139, 2148
 Ward W. R., 1981, *Icarus*, 46, 97
 Winter O. C. et al., 2009, *MNRAS*, 395, 218
 Yokoyama T., 1999, *Planet. Space Sci.*, 47, 619
 Yu Y., Baoyin H., 2012, *AJ*, 143, 62

This paper has been typeset from a Microsoft Word file prepared by the author.